Journal of Catalysis **204,** 314–323 (2001)
doi:10.1006/jcat.2001.3401, available online at http://www.idealibrary.com on IDEAL®

Function of Pd_n^0 Clusters, Pd^{2+}(oxo-) Ions, and PdO Clusters in the Catalytic Reduction of NO with Methane over Pd/MFI Catalysts

Bin Wen, Qi Sun, and Wolfgang M. H. Sachtler[1]

V. N. Ipatieff Laboratory, Center for Catalysis and Surface Science, Department of Chemistry, Northwestern University,
2137 Sheridan Road, Evanston, Illinois 60208

Received March 5, 2001; revised August 14, 2001; accepted August 14, 2001

Pd/MFI catalysts with a Pd/Al ratio ~1.0 were prepared by subliming $PdCl_2$ in a Cl_2-rich flow onto a H/MFI zeolite. Initially, $[PdCl]^+$ ions are formed in cation exchange positions; after hydrolysis they are converted to oxo-ions, possibly $[Pd\text{-}O\text{-}Pd]^{2+}$. Virtually no protons are formed in this step; all positive charge is localized on Pd entities. In contrast, neutral PdO particles, mainly located at the external surface, predominate in calcined Pd/MFI that is prepared by ion exchange from aqueous solution. The reduction of NO with methane to N_2 over the Pd/MFI catalysts does not require intermediate oxidation to NO_2; on the contrary, O_2 lowers the reaction rate. PdO particles catalyze the nonselective oxidation of methane to CO_2. Under steady-state conditions a dynamic equilibrium appears to exist between various forms of Pd, including clusters of *metallic* palladium. These are the sites where methane is dissociatively chemisorbed. By consequence, the catalytic activity of prereduced catalysts for NO reduction is initially much higher than that of preoxidized or steady-state catalysts. To detect the presence of a finite amount of metallic Pd under steady-state conditions, H/D exchange between CH_4 and D_2 was used as a catalytic probe. Formation of CH_3D has been identified with an oxygen-rich $NO/O_2/CH_4/D_2$ feed of even $O_2/D_2 = 20$. © 2001 Elsevier Science

Key Words: **NO reduction by methane; Pd/MFI catalyst preparation from $PdCl_2$ vapor; methane activation on Pd^0 clusters in SCR; *in situ* detection of Pd^0 clusters; methane H/D exchange.**

1. INTRODUCTION

Metal-exchanged zeolite catalysts are known to be active in the selective catalytic reduction (SCR) of NOx by hydrocarbons (1–4). For exhausts from gas engines or turbines fueled with natural gas the reduction of NO with CH_4 is an attractive strategy (5–6). Pd-exchanged H/MFI catalysts have been shown to be highly active converting NO with CH_4 to environmentally benign N_2 in the presence of O_2 (7–17). At least two reactions are involved:

$$2NO + CH_4 + O_2 \rightarrow CO_2 + N_2 + 2H_2O \qquad [1]$$

$$CH_4 + 2O_2 \rightarrow CO_2 + 2H_2O. \qquad [2]$$

There is a consensus in the literature that PdO clusters mainly catalyze the undesirable combustion reaction [2]. One obvious role of zeolite protons, therefore, is to dissipate PdO clusters into Pd^{2+} ions by "protonolysis." Arguments for this were presented in (12), but this effect of acidity on Pd dispersion under reaction conditions was discarded by Gélin *et al.* (18). Loughran and Resasco (7) argue that acidity is not only essential for metal dispersion, but also directly involved in a bifunctional reaction mechanism. Recent results of Kato *et al.* (10) and Koyano *et al.* (11) are consistent with this view. Aylor *et al.* proposed that positive $H^+(PdO)H^+$ions associated to two negatively charged Al centered tetrahedra are formed (19). In a more recent paper by Lobree *et al.* the model was slightly modified on the basis of density functional calculations; a hydroxo-ion $[Pd(OH)]^+$ associated to a proton is assumed to compensate the negative charges of two Al-centered tetrahedra (20). Ogura *et al.* (15) have tried to determine the fraction of Pd present as Pd^{2+} and found it essentially unchanged upon exposure to the reactant mixture, whereas Okumura *et al.* (21) assume that the local structure and the valence of palladium change significantly during NO adsorption or reaction of SCR of NO with CH_4.

Much less attention has been given to another potential player in this game: Pd_n^0 clusters, which are formed by reduction of either PdO clusters or Pd^{2+} ions. As the overall atmosphere in mixtures containing an excess of O_2 is oxidizing, most authors have considered Pd^0 merely as a precursor of the latter species, but disregarded their presence in the steady state of NO_x-SCR. Lobree *et al.* state that $H^+[Pd(OH)]^+$adducts are reduced above 337°C in the absence of O_2, but no reduction to Pd^0 is assumed when O_2 is present (20). One could argue, however, that under conditions where NO is reduced to N_2, it is not unlikely that part of PdO or of the oxo-ions of Pd will also be reduced

---

[1] To whom correspondence should be addressed. Fax: (847) 467-1018. E-mail: wmhs@northwestern.edu.

0021-9517/01 $35.00

to Pd^0, so that finite concentrations of zero-valent Pd may be present in a dynamic equilibrium. Both NO and CH_4 are potential reductants for PdO and oxo-ions. Indeed, recent results by Kato *et al.* (10) can be rationalized by assuming that activation of CH_4 on Pd atoms may be one of the rate-determining steps.

It is well known that methane is dissociatively chemisorbed on transition metals, with Rh and Pd having the lowest activation barrier for breaking the C-H bond. On a single metal atom a value of 16 kcal/mol has been calculated for Pd and 14 kcal/mol for Rh; this dissociation barrier is further lowered dramatically to 4–6 kcal/mol for Pd_2 (22). The main objective of the present study is to check whether Pd metal clusters are catalytically significant in the activation of methane over Pd/MFI catalysts, even in an excess of O_2 over CH_4.

In view of this objective it appears desirable to the use a preparation technique for Pd/MFI catalysts that leads to a higher Pd loading than is possible with ion exchange from aqueous solution, while the formation of PdO particles should be minimized. PdO particles that are present in catalysts prepared by incipient wetness impregnation are obviously undesirable because they are known to catalyze combustion of hydrocarbons.

These considerations led us to use a different preparation technique based on chemical vapor decomposition. Based on our experience from previous work with Fe/MFI and Co/MFI catalysts (23), it was decided to direct a beam of $PdCl_2$ vapor onto the H form of the MFI zeolite in order to carry out the reaction

$$PdCl_2 + H^+ \rightarrow [PdCl]^+ + HCl. \qquad [3]$$

However, the sublimation pressure of Pd halides is lower than that of $FeCl_3$ or $CoBr_2$; moreover dissociation of $PdCl_2$ molecules in the vapor phase is anticipated. Therefore, our "sublimation method" had to be modified and it was decided to sublime $PdCl_2$ in an atmosphere of Cl_2 onto solid H/MFI.

Summarizing, the primary objective of the present study is to determine the role of Pd_n^0 metal clusters in a Pd/MFI catalyst with high Pd loading, while the gas atmosphere is typical of NO reduction in emissions from lean burn engines. This requires some information on the dynamic interplay between Pd_n^0 clusters, isolated Pd^{2+} ions, Pd oxo-ions, and PdO clusters in a Pd/MFI catalyst at reaction temperature and exposed to an atmosphere of NO, CH_4, and an excess of O_2. A secondary objective is to compare Pd/MFI catalysts prepared by this sublimation with those prepared by conventional ion exchange. In particular, it is anticipated that the relative concentrations of protons, Pd^{2+} ions, and Pd oxo-ions will depend on the catalyst preparation technique.

2. EXPERIMENTAL

2.1. *Catalyst Preparation*

Pd/MFI catalysts were prepared by a modification of the sublimation method previously developed in this lab for the preparation of zeolite supported gallium, rhodium, iron, and cobalt (23–25). For comparison wet ion exchange was also used. H/MFI was obtained by three-fold ion exchange of Na/MFI (Si/Al = 23, UOP) with a diluted NH_4NO_3 solution to the NH_4^+ form at ambient temperature, followed by calcination in UHP O_2 flow at 550°C for 4 h.

$PdCl_2$ (Aldrich) was used for sublimation of its vapor onto H/MFI, followed by diffusion through the zeolite channels. The procedure is similar to that reported for Fe/MFI and Co/MFI (23), but for Pd/MFI 25% (volume) of Cl_2 gas was added to the Ar flow, in order to prevent decomposition of $PdCl_2$ vapor. The temperature was kept at 500°C; after 168 h, the sample was cooled down to 300°C in $Ar + Cl_2$, then the gas flow was replaced by $Ar + O_2$ to purge for 4 h. Subsequently, 30% H_2O vapor in Ar was used with a total flow rate of 60 ml/min to remove the chloride from the catalyst at 100°C. Condensing the off-gas in water and titration with $AgNO_3$ confirmed that the catalyst releases most of its chloride in this step. These catalysts will further be called SUB.

Ion exchange at room temperature of a dilute $(NH_3)_4Pd(NO_3)_2$ solution with H/MFI was used to prepare the samples further called WIE. After the slurry was stirred for 72 h, the slurry was vacuum filtered, the solid was washed thoroughly with DDI water, dried at 120°C in air, and calcined under flowing O_2, while the temperature was increased from 23 to 500°C with a linear ramp of 0.5°C/min.

Elemental analysis via inductively coupled plasma spectroscopy gives the following compositions relative to Al (atomic ratio):

SUB: $Pd/Al = 0.98 \quad Si/Al = 23 \quad Na/Al = 0$
WIE: $Pd/Al = 0.33 \quad Si/Al = 23 \quad Na/Al = 0.$

2.2. *Catalytic Tests*

Catalytic tests were carried out in a continuous flow tubular fixed bed micro-reactor as described previously (26). A 50-mg powder Pd/MFI sample was packed into the quartz reactor with a porous frit. The composition of the feed gas was regulated by mass-flow controllers (UNIT Instrument, URS-100). A typical feed contains 1000 ppm NO, 2000 ppm CH_4, and 2% O_2 with ultra-high purity He as diluent. The total flow rate was 150 ml/min (GHSV = 90,000 h^{-1}). The composition of the effluent was analyzed online by GC equipped with TCD. The conversion of NO was calculated from the formation of N_2 and that of CH_4 was determined from the amount of CO_2 in the effluent. Carbon monoxide and N_2O were never observed. Before starting a test one of two *in situ* treatments was applied. In one, the catalyst was heated in Ar and in the other, in O_2. The symbols SUB-Ar, WIE-Ar, SUB-O_2, and WIE-O_2 will further be used when referring to these catalysts. The temperature was ramped at 8°C/min from room temperature to 500°C, followed by holding at that temperature for 1 h, before adjusting it to the desired test temperature. A fresh sample was used at each temperature. The catalytic preference for NO reduction over methane combustion, Π_{NO}, is defined as

$$\Pi_{NO} = C(NO)/C(CH_4), \quad [4]$$

where C(NO) and $C(CH_4)$ stand for the conversions of NO and CH_4, respectively.

The feed gas always consisted of NO, CH_4, and O_2 except for the runs with an oxygen-free feed; in these runs O_2 was replaced by He after steady-state conversion was attained.

2.3. CH_4 Exchange with D_2 over the Samples

H/D exchange was carried out in a flow reactor and monitored by mass spectrometry (Gas Analyzer, Dycor M200 Quadrupole). A 50-mg sample was loaded in the reactor. Prior to the H/D exchange, the sample was pretreated *in situ* in O_2 while the temperature increased from 23 to 500°C with a ramp of 8°C/min, followed by a constant temperature of 500°C for 1 h (SUB-O_2, WIE-O_2). Subsequently, the temperature was lowered or raised (8°C/min) to the specified value and the sample was purged with He for 1 h. Subsequently, a mixture of 1000 ppm CH_4 (1% CH_4/He) and 1000 ppm D_2 (1% D_2/Ar) with He balance and a total flow rate of 80 ml/min was introduced into the system. These gases had been purified by MnO and 5 A molecule sieve traps to remove traces of O_2 or H_2O. Signal intensities were normalized by using the Ar^{2+} peak (M/e = 20) as an internal standard.

In order to investigate whether H/D exchange does take place under standard test conditions of NO_x SCR, 1000 ppm D_2 was added in some runs to the NO/CH_4/O_2 reaction mixture at 400°C after steady state had been attained.

2.4. Temperature Programmed Oxidation Studies

After CH_4-TPR or some catalytic tests the catalysts were oxidized in a temperature programmed oxidation (TPO). A continuous flow of 1% O_2/He (60 ml/min) was used for this purpose while the temperature was increased linearly (8°C/min). This reaction was conducted in a quartz fixed bed reactor. The gas products were monitored online by a Dycor M200 quadruple mass spectrometer.

2.5. Catalyst Characterization

Infrared spectra were obtained with a Nicolet 60 SX FTIR spectrometer, equipped with a liquid N_2 cooled mercury cadmium tellurid detector. Each sample was pressed into a self-supporting wafer with a diameter of 13 mm and a mass of 10 mg. The wafer was inserted into a quartz cell sealed with NaCl windows connected to the gas manifold. The sample was calcined *in situ* at 450°C in O_2 flow of 100 ml/min for 1 h and then cooled to room temperature in the same flow. All spectra were recorded at room temperature and 64 scans were accumulated with a spectral resolution of 1 cm^{-1}.

XRD patterns were recorded on a Rigaku diffractometer using Cu Kα radiation at 40 kV and 20 mA. Scanning started from 10 to 50° using steps of 0.05° with a counting time of 4.0 s.

H_2-TPR experiments were performed with an H_2/Ar (5%) flow of 40 ml/min from −80 to 500°C with a ramp of 8°C/min. The samples were pretreated in pure O_2 or Ar at 500°C for 1 h. The H_2 consumption was determined by a TCD detector, with H_2O being trapped in a dry ice cold trap. A similar procedure was used for CH_4-TPR with a CH_4/Ar (1%) flow, and the evolved products were monitored by mass spectrometry. CuO/SiO_2 (quartz) was used as a standard to calibrate the consumption of H_2 and the formation of CO_2.

3. RESULTS

XRD patterns of the SUB, WIE catalysts, and the parent H/MFI are shown in Fig. 1. The WIE catalyst shows a strong peak at $2\theta = 33.9°$, typical for the [101] plane refraction of PdO, indicating the presence of large PdO particles. This peak is absent in SUB. The peak at $2\theta = 40°$, known to be indicative for the [111] plane of Pd metal is absent in all samples. No significant changes in the zeolite refractions are caused by the presence of the palladium.

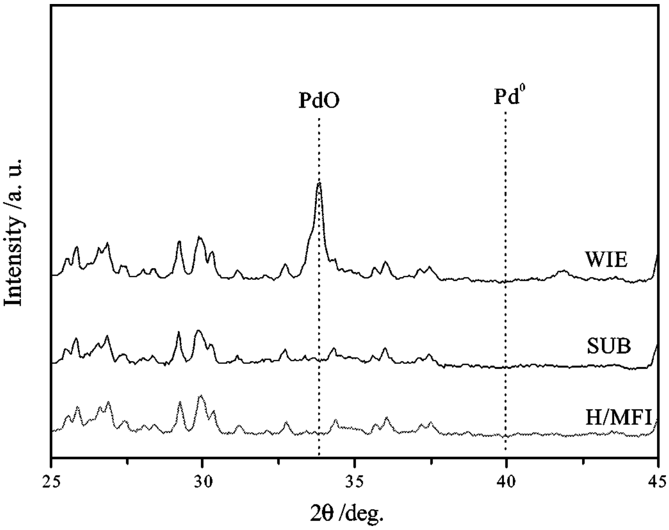

FIG. 1. XRD patterns of WIE and SUB as well as H/MFI. PdO: (101) line of Pd oxide, Pd^0: (111) line of metallic Pd.

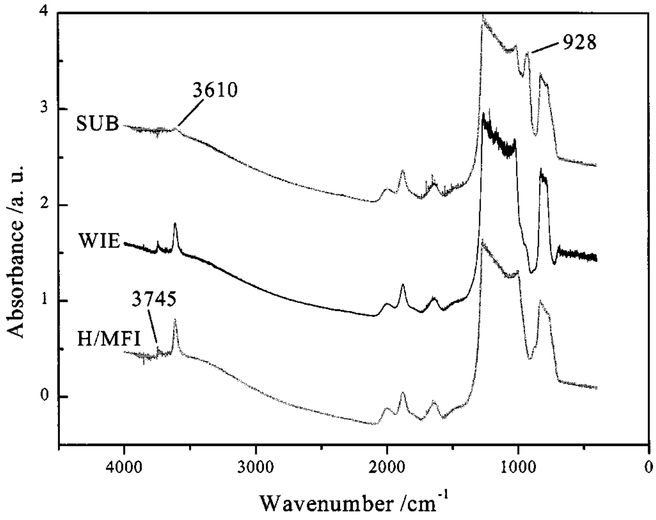

FIG. 2. FTIR spectra of WIE and SUB and of the H/MFI precursor.

The infrared spectra of the samples are shown in Fig. 2. For H/MFI, a weak band at 3745 cm^{-1} and a strong band at 3610 cm^{-1} are attributed to isolated and terminal silanol groups (27) and acidic bridging hydroxyl groups (28), respectively. Peak integration reveals that in WIE only 3% of the original Brønsted sites have been replaced by Pd^{2+} ions. This means that about 8% of the palladium in WIE exists as Pd^{2+} ions, the remainder as PdO. In SUB, the bands at 3610 and 3745 cm^{-1} have become very weak, indicating that most of the Brønsted acid sites have been replaced by Pd^{2+} ions. Apparently $PdCl_2$ vapor reacts not only with the strong acid sites, but also with silanol groups. Over SUB, the band at 928 cm^{-1} shows that Pd interaction with its oxygen neighbors induces a severe perturbation of the zeolite vibrations (29–32).

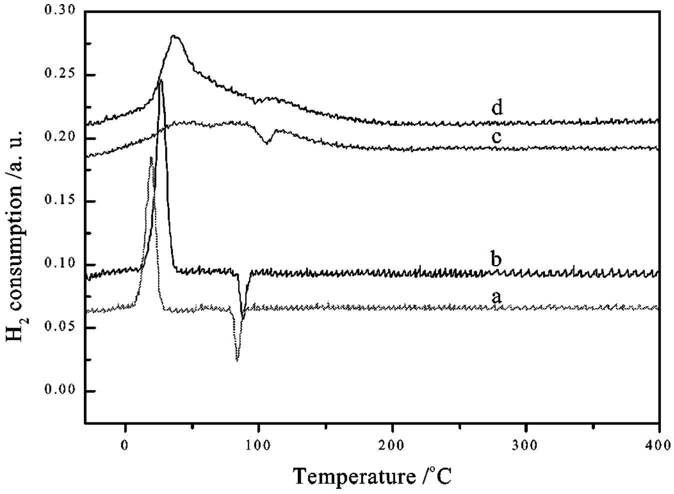

FIG. 3. TPR profiles of (a) WIE-Ar, (b) WIE-O_2, (c) SUB-Ar, and (d) SUB-O_2.

Figure 3 shows the H_2-TPR profiles. The differences between WIE and SUB are quite significant. For WIE (traces (a) and (b)), the TPR profiles fall in two groups: peaks near 20°C are sharp and ascribed to the reduction of PdO particles. This assignment is confirmed by the absence of this peak in the sample that was prereduced with CO at 400°C. Negative peaks near 80°C are characteristic of the decomposition of the Pd-β-hydride (33–35); their presence confirms that Pd_n^0 has been formed by the reduction of PdO (12, 36). No peaks characteristic for the reduction of Pd^{2+} ions are observed in WIE. Traces (c) and (d) are the H_2-TPR profiles of SUB-Ar and SUB-O_2. The peaks of the SUB samples are much broader than those of the WIE catalysts. The H_2 consumption peak between –30 and 180°C indicates reduction of Pd^{2+} ions or oxo-ions. Remarkably, no band at 3610 cm^{-1} is detected with the calcined SUB catalysts. This absence of acidic protons implies that palladium entities are carriers of the positive charge. This is indeed confirmed by the FTIR spectrum in the region typical for the zeolite lattice vibrations (Fig. 2). Peak integration of the profiles in Fig. 3 shows that for the samples pretreated in O_2, the total H_2 consumption corresponds to a molar ratio of $H_2/Pd = 1.0$. This proves that in these catalysts all the palladium is present as divalent Pd and that it is quantitatively reduced to Pd^0 during H_2-TPR. In contrast, for samples that were heated in Ar, the H_2/Pd ratio is only 0.61 for the SUB and 0.77 for the WIE catalyst. This shows that part of the Pd is thermalyl reduced to Pd^0. It is also noteworthy that the negative peaks, typical of the β-hydride decomposition, have different sizes. This indicates a different extent of aggregation in Pd_n^0.

As usual, the CH_4 conversion increases monotonically with temperature over both catalysts, but the NO reduction to N_2 passes through a maximum over all catalysts. In the ascending branch the NO reduction activity is higher for the SUB preparations, whereas the methane combustion is higher for the WIE catalysts (not shown). This result is in conformity with the higher PdO content of the WIE preparations.

The effect of catalyst pretreatment on the catalytic performance at a constant temperature of 300°C is depicted in Fig. 4. Clearly, SUB-Ar, known to contain some reduced Pd, displays higher NO reduction activity than SUB-O_2. Obviously, the presence of Pd^0 favors high catalytic performance. Interestingly, this memory is observed for more than 8 min, which shows that oxidation of Pd^0 is not very fast at 300°C. The conclusion that this higher activity is due to Pd^0 is confirmed by a test with a SUB catalyst that was prereduced at 300°C for 20 min in 5% H_2/Ar with a flow rate of 60 ml/min. This catalyst (SUB-H_2) displays a high initial NO conversion to N_2 of 35%; after 10 min it is still 17%.

Intensive reorganization of catalysts SUB-O_2 and SUB-Ar takes place at 400°C until a steady state is reached. During this period, CH_4 conversion to CO_2 passes through a

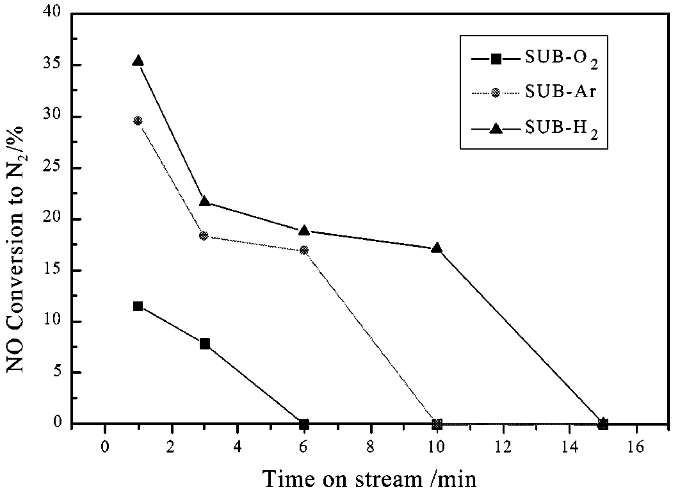

FIG. 4. Conversion of NO to N_2 at 300°C for three differently pretreated SUB catalysts, before steady state is attained.

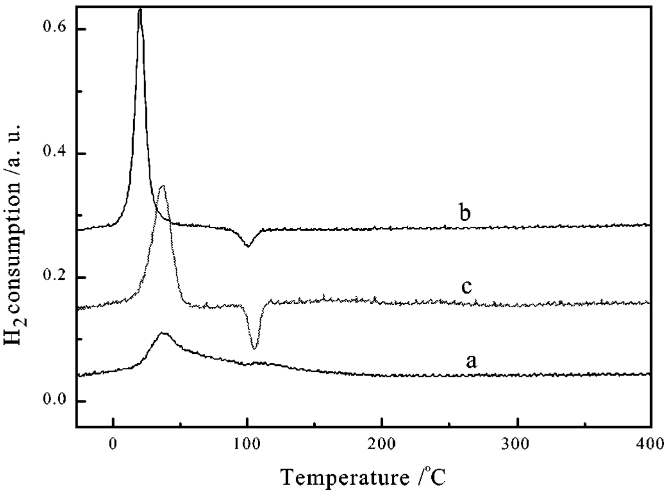

FIG. 6. TPR profiles of (a) fresh SUB-O_2, (b) after reduction/reoxidation treatment, (c) after exposure to NO-CH_4-O_2 at 400°C for 1 h.

deep minimum, while NO conversion to N_2 passes through a maximum. The NO preference, Π_{NO}, calculated from these data, is plotted in Fig. 5. Clearly, the SUB-Ar catalyst containing Pd^0 is more selective than SUB-O_2 until memory of the different pretreatments vanishes.

The changes in the state of Pd caused by interaction with the feed under catalytic conditions, are illustrated by the TPR profiles in Fig. 6. Three profiles characterize (a) the fresh SUB-O_2 catalyst, (b) the same after reduction with H_2 at 300°C for 10 min, followed by oxidation with O_2 at 500°C for 1 h, and (c) after reaction of NO-CH_4-O_2 at 400°C for 1 h. Evidently, the reduction/reoxidation sharpens the H_2 consumption peak and shifts it downward. Independent calibration with PdO/SiO_2 confirms that the peak in trace (b) is due to PdO particles. It follows that treatment with H_2 reduces the divalent Pd to Pd_n^0 clusters, and subsequent oxidation converts them to PdO particles. This observation is in line with our previous work (12). After exposure to the reaction mixture for 1 h, a TPR peak is observed, which is located near that of fresh SUB-O_2, but without the "tail" of profile (a).

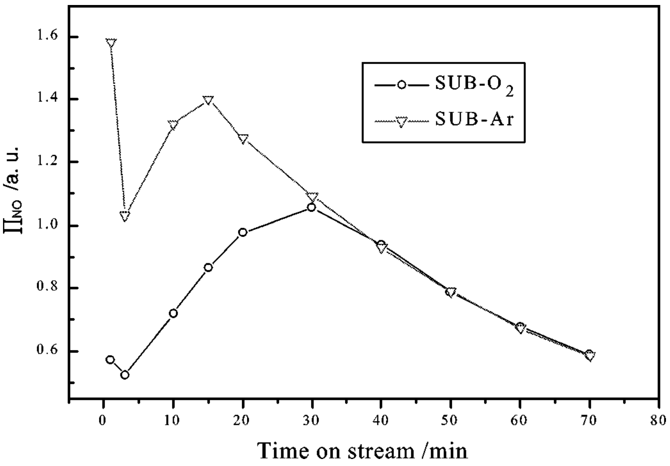

FIG. 5. The catalytic preference for NO reduction over methane combustion over SUB-O_2 and SUB-Ar at 400°C before reaching steady state.

The influence of O_2 on NO reduction was examined by replacing the standard $NO/CH_4/O_2$ feed, after steady-state conversion was attained at 400°C, by an O_2-free feed. The MS and GC data before and after this jump in feed composition are presented in Fig. 7. Clearly, the CH_4 peak increases and the CO_2 peak sharply decreases. While the mass spectrometer does not discriminate between CO and N_2 for $M/e = 28$, the decreasing $M/e = 30$ peak shows that more NO is converted in the absence of O_2 than in its presence. This result is confirmed by the GC analysis. After the jump to the O_2-free feed, the NO conversion increases within 5 min by a factor larger than 5.

Surprisingly, also H_2 is detected upon using an O_2-free feed. This suggests that Pd^0 particles are formed and methane dissociates at their surface. The results leave little doubt that CH_4 and/or NO efficiently reduces PdO particles at 400°C creating sites where CH_4 dissociates.

Temperature programmed reduction with CH_4 leads to the CH_4-TPR profiles shown in Fig. 8. With the WIE-O_2 catalyst CH_4 consumption between 200 and 250°C reveals reduction of PdO and formation of $CO_2 + H_2O$. These peaks are absent over SUB-O_2, confirming again the absence of significant amounts of PdO in this preparation. However, some consumption of CH_4 is detected between 350 to 400°C and CO is formed identified by the $M/e = 28$ peak. After the Pd in the SUB-O_2 catalyst is converted to PdO by the reduction/reoxidation treatment, the TPR profile in Fig. 8c shows a broad CH_4 consumption peak between 200 and 300°C, and concomitant formation of CO_2 and H_2O. At higher temperatures, large amounts of H_2 are

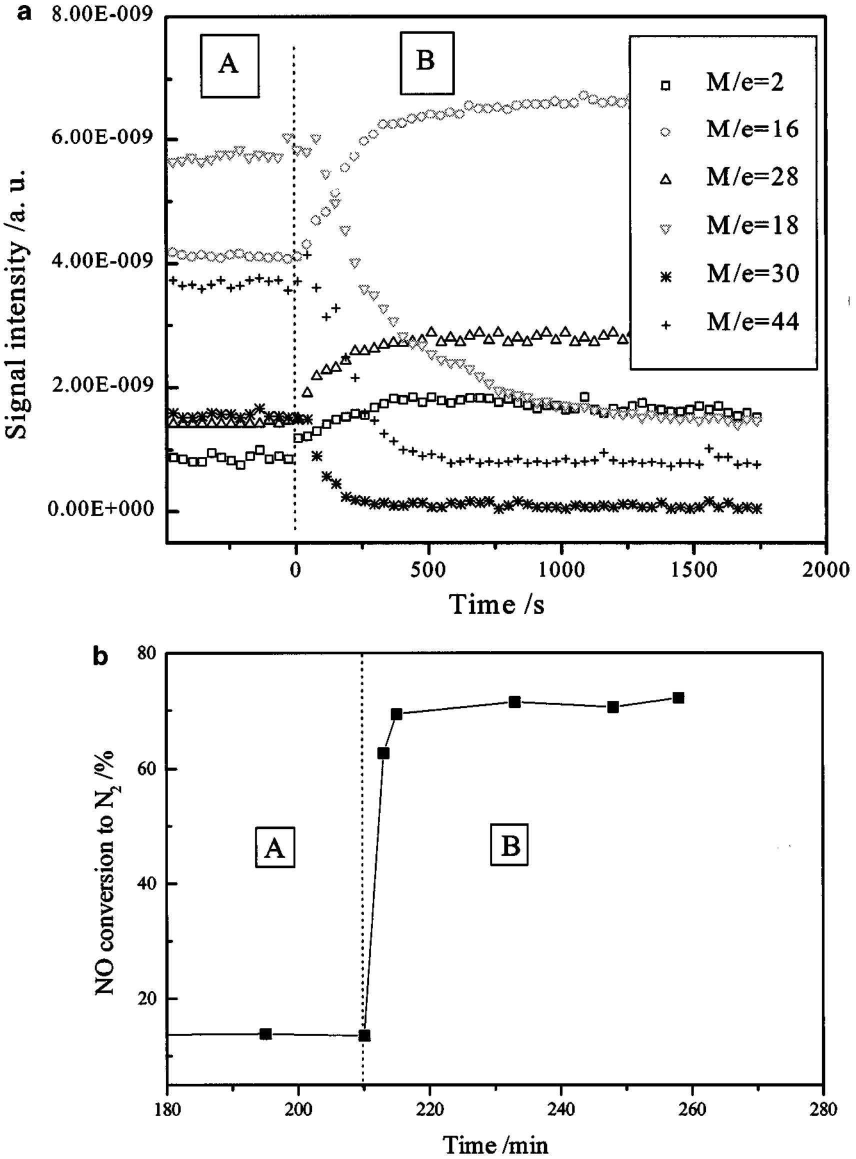

FIG. 7. The effects of oxygen on the catalytic performance of SUB-Ar or SUB-O_2 at 400°C, GHSV = 90,000 h^{-1}. (a) MS data; (b) GC data. A, in steady state of NO-CH_4-O_2 reaction; B, after O_2 is replaced by He.

formed on all three samples, indicating, again, the presence of Pd metal. Meanwhile, a small amount of C_2H_4 is also observed. Note that the H_2, which is formed by CH_4 decomposition, will of course, swiftly reduce Pd^{2+} ions to Pd metal, and protons are formed (12).

Reoxidation by TPO of the catalysts that had been subjected to CH_4-TPR results in significant O_2 consumption above 450°C and formation of a large amount of CO_2 and also some CO. This confirms the deposition of carbonaceous material when methane decomposes on the surface of Pd_n^0 clusters. The TPO results also show that high temperature is needed to remove the surface carbonaceous deposits. However, if the CH_4-TPR was carried out only below 450°C, a more reactive deposit is formed which is oxidized to CO_2 near 200°C. This confirms the well-known fact that "soft coke" is formed at low temperatures, but "hard coke" at high temperatures when hydrocarbons dissociate on transition metal surfaces. Interestingly, no CO or CO_2 evolution is detected in the TPO profile over the SUB-O_2 after exposure to NO-CH_4-O_2 for 1 h at 400°C. Apparently, little carbonaceous deposit is formed during the SCR reaction over this catalyst.

Exposure of SUB-O_2 to a flow of $CH_4 + D_2$ at 400 °C reduces the Pd and initiates H/D exchange of CH_4. Figure 9 shows the MS signals for H_2, HD, CH_3D (M/e = 17), CH_2D_2 (M/e = 18), CHD_3 (M/e = 19), which increase to a steady-state level. Simultaneously, the M/e = 16 signal of CH_4 decreases, indicating CH_4 consumption. The absence

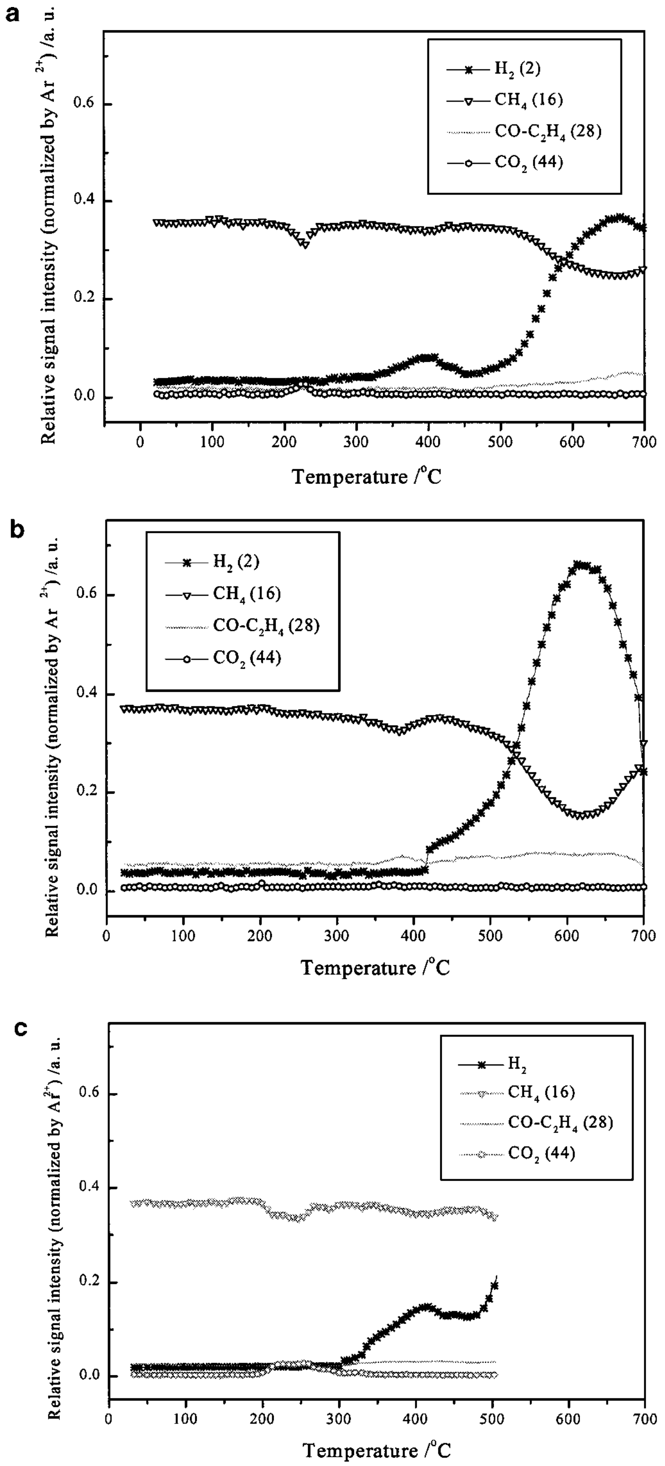

FIG. 8. CH_4-TPR profiles of (a) WIE-O_2, (b) SUB-O_2, (c) SUB after H_2 reduction, and O_2 reoxidation as in Fig. 6b.

of CO (M/e = 28) or CO_2 (M/e = 44) eliminates the possibility that CH_4 reacts with oxygen impurities and confirms that H/D exchange is the sole reaction. Whereas residual water (H_2O, HDO, or D_2O) might cause signals at M/e = 18, 19, or 20, it appears safe to ascribe the M/e = 17 signal to CH_3D, because the OH^+ fragment ion of H_2O and HDO is known to have an extremely low intensity (37). The formation of CH_3D is thus taken as proof for the presence of Pd_n^0 clusters. The activity of SUB-O_2 for H/D exchange is found to be significant even at a temperature as low as 250°C.

To probe for the presence of Pd^0 even under the conditions of NO reduction, the SUB-O_2 catalyst was first exposed to the standard NO/CH_4/O_2 feed. After steady state is established, a small amount of D_2 was added to the feed gas while keeping the GHSV constant. As seen in Fig. 10, this D_2 addition has no significant effect on the NO conversion. However, the M/e = 17 signal increases rapidly and becomes constant within 5 min while the M/e = 19 signal increases gradually. This confirms that H/D exchange of CH_4 takes place even under NO-SCR conditions. Additional data show that any contribution of an OH^+ peak

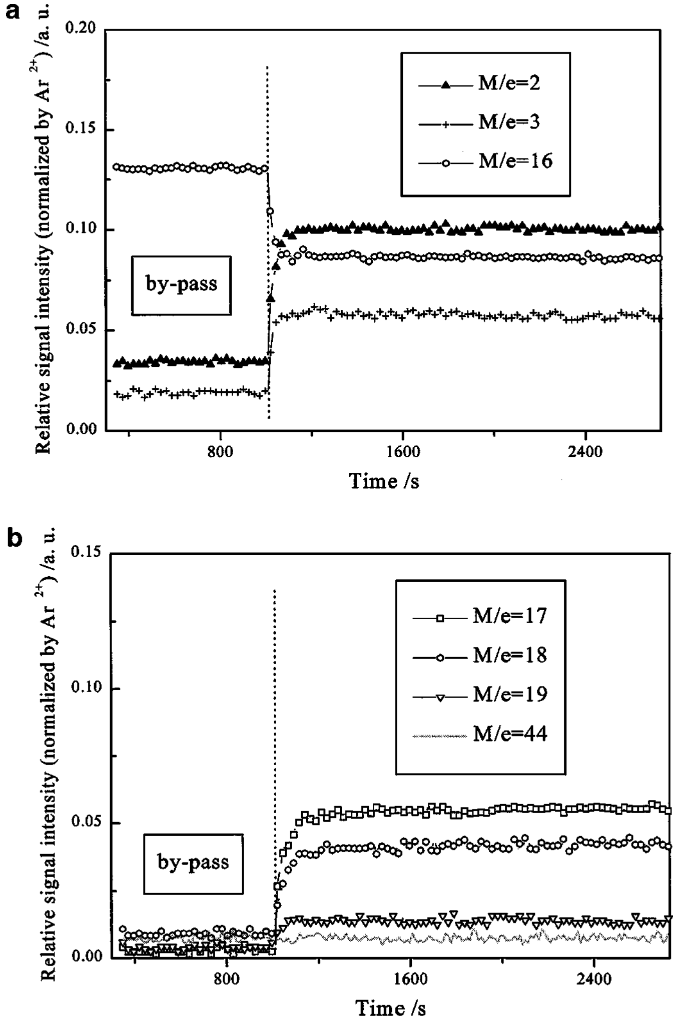

FIG. 9. Time dependence of the signal intensity upon the H/D exchange reaction of CH_4 over SUB-O_2. CH_4 1000 ppm, D_2 1000 ppm, GHSV = 48,000 h^{-1}, temperature 400°C.

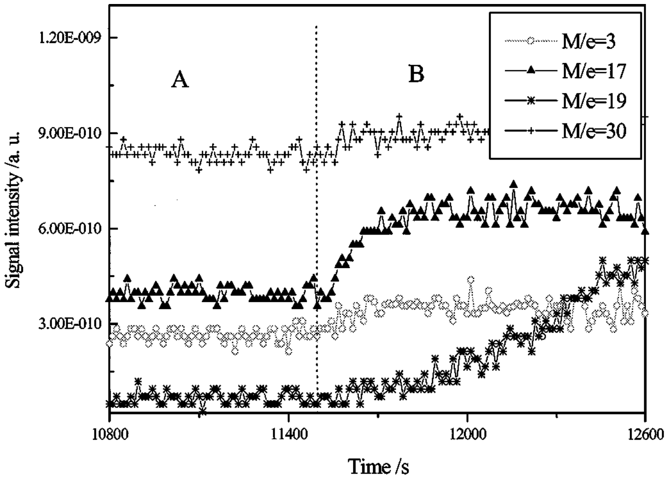

FIG. 10. Effect of introducing 1000 ppm of D_2 into the NO-CH_4-O_2 feed after steady state was obtained at 400°C and GHSV = 90,000 h^{-1}. NO: 1000 ppm, CH_4: 2000 ppm, O_2: 2%. A, in steady state of NO-CH_4-O_2 reaction; B, after D_2 is introduced into the reaction system.

to the M/e = 17 signal will be lower than 40% of the observed intensity of that peak.

4. DISCUSSION

4.1. General Remarks

The present data show that for NO reduction with methane over Pd/MFI is fundamentally different from that used for NO_x reduction with larger hydrocarbons over catalysts such as Cu/MFI, Fe/MFI, Co/MFI, or H/MFI + CeO_2 (38). This difference is clearly illustrated by the role of O_2: Over Cu/MFI and Fe/MFI the reaction order in O_2 is positive, the SCR rate is very low in the absence of O_2, but for the reduction of NO with methane over Pd/MFI the rate is much higher in an O_2-free feed. For a Pd/MFI catalyst prepared by ion exchange, Kato *et al.* (10) report the following reaction orders: $n(\mathrm{NO}) = 1.05$; $n(\mathrm{CH_4}) = +0.66$; $n(\mathrm{O_2}) = -0.26$. In contrast, it is well known that with Cu/MFI and Fe/MFI oxygen is required for NO oxidation to N_2O_3, NO_2, or even NO_3^- ions; no such oxidation is apparently needed over Pd/MFI.

The present data also confirm another phenomenon, not unusual in heterogeneous catalysis: the first stage of the catalytic process is actually the last stage of catalyst preparation. Important reorganizations take place inside the catalyst upon its first contact with all reactants and products at reaction temperature.

The present work shows that it is possible to prepare Pd/MFI by deposition of $PdCl_2$ vapor on H/MFI, provided that Cl_2 gas at a sufficient pressure is added to shift the equilibrium

$$\mathrm{PdCl_2} = \mathrm{Pd^0} + \mathrm{Cl_2} \qquad [5]$$

to the left. The procedure requires hundreds of hours but results in a catalyst of high Pd loading and initially, low content of Pd oxide particles. A Pd loading corresponding to Pd/Al = 0.98 is readily achieved with this "sublimation method," whereas with wet ion exchange it is difficult to even approach the theoretical limit of Pd/Al = 0.5. With the WIE samples tested in the present work, a ratio of only Pd/Al = 0.33 was achieved.

4.2. Possible States of Pd in As-Prepared and Steady-State Catalysts

The number of negative charges in a zeolite is given by the number of Al-centered tetrahedra and remains constant upon adding palladium and replacing Cl^- by OH^- ions with the methods described in this paper. This negative charge should be equal to the sum of positive charges of protons and palladium entities. As the concentration of protons can be determined from the band intensity of the 3610 cm^{-1} band, the charge on the Pd at any stage can be derived from the intensity difference of this band in the parent H/MFI zeolite and the Pd/MFI catalyst.

In WIE, most of the Pd is present after calcination as aggregated PdO particles at the external surface of the zeolite. The XRD refraction line typical for PdO and the sharp H_2-TPR peak below 50°C in traces (a) and (b) of Fig. 3 show this unambiguously. A high concentration of protons compensates the negative charge of the zeolite lattice. In contrast, the calcined SUB catalyst contains no PdO detectable by XRD and no sharp H_2-TPR peak. The virtual absence of the IR band at 3610 cm^{-1} in Fig. 2 proves that the positive charge necessary to compensate the zeolite lattice charge is localized on some Pd entities. They replace the original Brønsted acid sites (and even part of the protons in silanol groups) and will be located at or very near the cation exchange sites of the zeolite. When desired, PdO particles can be created in the SUB catalyst by first reducing all Pd to Pd^0, then oxidizing the Pd metal to PdO. The sharp TPR peak in profile (b) of Fig. 6 shows the result of this operation; it can be used for internal calibration.

Charge balance in calcined SUB catalysts would be achieved if 50% of the Pd were present as Pd^{2+} ions and the other 50% as neutral PdO particles. However, the absence of any PdO detectable by XRD and TPR disproves this model. It follows that in the calcined SUB catalyst the majority of the Pd is present as oxo- or hydroxo-cations. Extra lattice anions ligated to Pd compensate roughly 50% of the charge of each Pd^{2+} ion. Another criterion for the presence of positively charged Pd-oxo-ions is the lattice perturbation band at 928 cm^{-1}. For Cu/MFI, Fe/MFI, and Co/MFI it is known that (oxo-) ions of transition metals strongly interact with zeolite oxygens and give rise to such perturbation of the lattice vibration in this region of the IR spectrum. In contrast, neutral oxide particles lack that propensity (29–32).

Several models are conceivable for the oxo- or hydroxo-ions of Pd in cation exchange sites of the zeolite. In particular, two models come to mind: (a) $H^+(PdO)H^+$, as proposed by Aylor *et al.* (19) for Pd/MFI catalysts of much lower metal loading; (b) oxygen bridged binuclear $[Pd\text{-}O\text{-}Pd]^{2+}$, analogous to the well-known $[Cu\text{-}O\text{-}Cu]^{2+}$ ions, generally accepted for Cu/MFI catalysts, and the $[HO\text{-}Fe\text{-}O\text{-}Fe\text{-}OH]^{2+}$ model identified by EXAFS for Fe/MFI prepared by sublimation (40, 41).

A distinction between these models can be made by the combination of CO-TPR with FTIR. Both oxo-species should be reducible with CO. In the first model, this should lead to the formation of new Brønsted sites:

$$H^+(PdO)H^+ + CO \rightarrow CO_2 + Pd + 2H^+. \qquad [6]$$

No protons will be formed by CO-TPR if the second model is correct:

$$[Pd\text{-}O\text{-}Pd]^{2+} + CO \rightarrow CO_2 + Pd^{2+}\text{-}Pd^0. \qquad [7]$$

The present data show that no detectable FTIR band at 3610 cm^{-1}. It thus appears that for the SUB catalysts the binuclear model is closer to reality than the model of the mononuclear Pd-hydroxo-cation. The broad TPR profile of the calcined SUB catalyst in Fig. 3 indicates that the Pd, though clearly in the Pd^{2+} state, is not uniform but a variety of states coexist. A much sharper TPR peak is observed with the SUB sample after use as a catalyst (Fig. 6c). The position of this peak is clearly different from that of PdO particles obtained by reduction, followed by oxidation with O_2.

4.3. Dynamic Equilibrium between Various Valence States of Palladium.

The relative amounts of Pd^0 and Pd^{2+} in the steady state will be given by the respective rates of oxidation and reduction. Pd is known to easily chemisorb O_2 at very low temperature, for instance, Brennan *et al.* found a value of 67 kcal/mol for the initial heat of adsorption on Pd films (39). Oxidation of bulk Pd metal to PdO is exothermic by 42 kcal/mol but kinetically inhibited by slow outward diffusion of cations through the oxide layer. Such diffusion through an oxide layer will be less critical for small particles. The rate of reduction of Pd^{2+} to Pd^0 depends on the reductant and the state of the Pd^{2+}, whether it is present as isolated ions, mono- or binuclear oxo-ions, or as PdO particles. Comparison of SUB-O_2 and SUB-Ar in Fig. 3 shows that thermal reduction by mere heating in Ar at 500°C causes reduction of 39% of the Pd. The data in Fig. 6 show that H_2 reduces all forms of Pd^{2+} of interest here swiftly to Pd^0 at low temperatures. Other potential reductants are NO or CH_4 that are part of the feed and CO as a potential intermediate of NO reduction with methane. In preliminary work beyond the scope of the present paper we found that NO reduced part of PdO at very low temperatures by a process, which can be written in a simplified way as

$$2PdO + 2NO = Pd^0 + Pd(NO_2)_2. \qquad [8]$$

Traces (a) and (c) in Fig. 8 show that reduction of PdO with methane is significant above 200°C; for Pd oxo-ions it is clear from trace (b) that they are reduced by methane above 340°C. It follows from all these data that under the conditions of NO reduction with methane, Pd in MFI undergoes both oxidation and reduction processes.

The data in Figs. 4 and 5, obtained in nonsteady-state runs, clearly show that at low temperatures prereduced catalysts are much more active in catalyzing NO reduction to N_2 than preoxidized or steady-state catalysts. The selectivity for the desired reaction is initially higher for the thermally reduced catalyst SUB-Ar than for SUB-O_2. Under the SCR conditions a complicated reorganization of the solid takes place, until both catalysts show the same performance which further decreases with time. The content of Pd^0 will certainly be much lower in the steady state than in the initial prereduced catalyst, but oxidation of Pd^0 by the reaction mixture is certainly not an instantaneous process. It follows from these results that Pd^0 will have a significant and positive effect on the catalytic performance in NO-SCR. While PdO particles catalyze the undesired oxidation of hydrocarbons to CO_2, Pd metal will outperform all other ingredients of this catalyst in dissociating the C-H bond of methane. Previously, Blomberg *et al.* (22) showed that palladium clusters are very efficient at activating methane.

The crucial question remains, whether minute amounts of Pd^0 are still present and mechanistically significant in the steady state. Numerous physical methods exist to identify Pd metal, but most of them are not applicable for *in situ* identification of a very small number of Pd clusters in a working catalyst. Taking samples, cooling them in an atmosphere that is either reducing or oxidizing and then analyzing them for Pd^0 would not be adequate to prove that this Pd^0 was present (or absent) during the catalytic reaction. That is why in this work we have chosen to use a catalytic probe that can be truely applied *in situ.* The reaction

$$CH_4 + D_2 \rightarrow CH_3D + HD \qquad [9]$$

followed by formation of CH_2D_2, CHD_3, and CD_4, is known to be a very sensitive probe for the presence of transition metal clusters in the metallic state. Clearly, metallic palladium will also catalyze the formation of D_2O from O_2 and D_2, but if the rate of reaction [9] can compete with this process and some deuteromethane can be detected, this will be a very strong argument in favor of the presence of Pd metal clusters during the catalytic reduction of NO to N_2.

The run depicted in Fig. 9 confirms that the SUB-O_2 catalyst has the propensity to catalyze reaction [9]. The crucial experiment is, of course, the run in Fig. 10, where a small amount of D_2 was added to the NO-SCR feed. Clearly, even with a ratio of D_2/O_2 of only 1/20, a very significant formation of CH_3D (M/e = 17) is observed. In our opinion, these data prove that metallic palladium is indeed present in the working catalyst under SCR conditions.

5. CONCLUSIONS

Sublimation of $PdCl_2$ in a Cl_2 flow onto H/MFI results in Pd/MFI catalysts of much higher Pd loading, without concomitant formation of PdO particles, than ion exchange from aqueous solution. Thorough reorganizations inside the solid take place when a catalyst is first exposed to a flow of $NO + O_2 + CH_4$ at reaction temperature. Prereduced catalysts are initially much more active than preoxidized or steady-state catalysts. The dynamic equilibrium between catalyst reduction and catalyst oxidation steps results in a finite concentration of *metallic* Pd clusters in the presence of an excess of O_2 over CH_4. Pd^0 sites provide an efficient reaction path for NO SCR with methane by dissociating C-H bonds. Pd metal is identified *in situ* by using H/D exchange of CH_4 as a catalytic probe: even with a ratio of $D_2/O_2 = 0.05$ in the feed, formation of CH_3D and higher deuterated isotopomers of methane is detected.

The propensity of Pd/MFI and Co/MFI to catalyze NO SCR to N_2 with methane is in striking contrast to the inability of Cu/MFI and Fe/MFI to catalyze this reaction. The present results suggest that this difference is due to the formation in Pd/MFI and Co/MFI of surface sites which dissociate C-H bonds in CH_4.

ACKNOWLEDGMENTS

This work was supported by EMSI program of the National Science Foundation and the U.S. Department of Energy Office of Science (CHE-9810378) at the Northwestern University Institute for Environmental Catalysis. Financial aid from the Director of the Chemistry Division, Basic Energy Sciences, U.S. Department of Energy, Grant DE-FGO2-87ER13654, is gratefully acknowledged.

REFERENCES

1. Iwamoto, M., Yahiro, H., Yu-U, Y., Shundo, S., and Mizuno, N., *Shokubai* **32**, 430 (1990).
2. Li, Y., and Armor, J. N., *Appl. Catal. B* **1**, L31 (1992).
3. Li, Y., and Armor, J. N., *Appl. Catal. B* **2**, 239 (1993).
4. Burch, R., and Scire, S., *Appl. Catal. B* **3**, 295 (1994).
5. Armor, J. N., *Catal. Today* **26**, 147 (1995).
6. Hamada, H., *Catal. Today* **22**, 21 (1994).
7. Loughran, C. J., and Resasco, D. E., *Appl. Catal. B* **7**, 113 (1995).
8. Ali, A., Alvarez, W., Loughran, C. J., and Resasco, D. E., *Appl. Catal. B* **14**, 13 (1997).
9. Nishizaka, Y., and Misono, M., *Chem. Lett.* 2237 (1994).
10. Kato, H., Yokoyama, C., and Misono, M., *Catal. Today* **45**, 93 (1998).
11. Koyano, G., Yokoyama, S., and Misono, M., *Appl. Catal. A* **188**, 301 (1999).
12. Adelman, B. J., and Sachtler, W. M. H., *Appl. Catal. B* **14**, 1 (1997).
13. Descorme, C., Gélin, P., Primet, M., and Lécuyer, C., *Catal. Lett.* **41**, 133 (1996).
14. Descorme, C., Gélin, P., Lécuyer, C., and Primet, M., *J. Catal.* **177**, 352 (1998).
15. Ogura, M., Hayashi, M., Kage, S., Matsukata, M., and Kikuchi, E., *Appl. Catal. B* **23**, 247 (1999).
16. Uchida, H., Yamaseki, K., and Takahashi, I., *Catal. Today* **29**, 99 (1996).
17. Ohtsuka, H., and Tabata, T., *Appl. Catal. B* **21**, 133 (1999).
18. Gélin, P., Goguet, A., Descorme, C., Lécuyer, C., and Primet, M., *in* "Proceedings, 4th International Congress on Catalysis and Automotive Pollution Control, Brussels, 1997," Vol. 2, p. 197.
19. Aylor, A. W., Lobree, L. J., Reimer, J. A., and Bell, A. T., *J. Catal.* **172**, 453 (1997).
20. Lobree, L. J., Aylor, A. W., Reimer, J. A., and Bell, A. T., *J. Catal.* **181**, 189 (1999).
21. Okumura, K., Amano, J., Yasunobu, N., and Niwa, M., *J. Phys. Chem. B* **104**, 1050 (2000).
22. Blomberg, M. R. A., Siegbahn, P. E. M., and Svensson, M., *J. Phys. Chem.* **96**, 5783 (1992).
23. Wang, X., Chen, H.-Y., and Sachtler, W. M. H., *J. Catal.* **107**, 281 (2001).
24. Kwak, B. S., and Sachtler, W. M. H., *J. Catal.* **141**, 729 (1993).
25. Feeley, O. C., and Sachtler, W. M. H., *Appl. Catal.* **75**, 93 (1991).
26. Chen, H.-Y., and Sachtler, W. M. H., *Catal. Today* **42**, 73 (1998).
27. Zecchina, A., Bordiga, S., Spoto, G., Marchese, L., Petrini, G., Leofanti, G., and Padovan, M., *J. Phys. Chem.* **96**, 4991 (1992).
28. Chester, A. W., Dessan, R. M., Alemani, L. B., and Woolery, G. L., *Zeolites* **6**, 14 (1986).
29. Sárkány, J., and Sachtler, W. M. H., *Zeolites* **14**, 7 (1994).
30. Sárkány, J., and Sachtler, W. M. H., *Stud. Surf. Sci. Catal.* **94**, 649 (1995).
31. Lei, G. D., Adelman, B. Sárkány, J., J., and Sachtler, W. M. H., *Appl. Catal. B* **5**, 245 (1995) .
32. Chen, H.-Y., Wang, X., and Sachtler, W. M. H., *Phys. Chem. Chem. Phys.* **2**, 3083 (2000).
33. Homeyer, S. T., and Sachtler, W. M. H., *Appl. Catal.* **54**, 189 (1989).
34. Boudart, M., and Hwang, H. S., *J. Catal.* **39**, 44 (1975).
35. Lieske, H., and Völter, J., *J. Phys. Chem.* **89**, 1841 (1985).
36. Homeyer, S. T., and Sachtler, W. M. H., *J. Catal.* **117**, 91 (1989).
37. Stenhagen, E., Abrahamsson, S. F., and McLafferty, W., "Atlas of Mass Spectral Data." Interscience, New York/London, 1969.
38. Liese, T., Löffler, E., and Grünert, W., *J. Catal.* **197**, 123 (2001).
39. Brennan, D., Hayward, D. O., and Trapnell, B. M. W., *Proc. Roy. Soc. A* **256**, 81 (1960).
40. Marturano, P., Drozdová, L., Kogelbaur, A., and Prins, R., *J. Catal.* **192**, 236 (2000).
41. Battiston, A. A., Bitter, J. H., Koningsberger, D. C., *Catal. Lett.* **66**, 75 (2000).